

Synthesis of Gallium–Aluminum Dawsonites and their Crystal Structures

Tsunenori Watanabe,^{‡,§} Takeo Masuda,[‡] Yoshihisa Miki,[‡] Yuya Miyahara,[‡] Hyung-Joon Jeon,[‡] Saburo Hosokawa,[‡] Hiroyoshi Kanai,[‡] Hiroshi Deguchi,[§] and Masashi Inoue^{*,‡,‡}

[‡]Department of Energy and Hydrocarbon Chemistry, Graduate School of Engineering, Kyoto University, Katsura, Kyoto 615-8510, Japan

[§]Power Engineering R&D Center, The Kansai Electric Power Company Inc., 3-11-20, Nakoji, Amagasaki 661-0974, Japan

Solid solutions of dawsonites, ammonium aluminum carbonate hydroxide–ammonium gallium carbonate hydroxide, were obtained by the addition of aqueous solutions of mixtures of aluminum and gallium nitrates to an excess ammonium carbonate solution. The dawsonite solid solutions were calcined at 700°C to give γ -Ga₂O₃–Al₂O₃ solid solutions. The structures of these two types of solid solution were discussed on the basis of their X-ray diffraction patterns and X-ray absorption fine structure spectra.

I. Introduction

GALLIUM OXIDE has unique catalytic functions for dehydrogenation of paraffins,^{1,2} isomerization of hydrocarbons,³ nitrogen oxide reduction with hydrocarbons,^{4–7} decomposition of CF₄,⁸ and epoxidation of olefins with hydrogen peroxide.⁹ It also has photocatalytic activity^{10,11} and exhibits interesting support effects on the performance of noble metal^{12–16} and Ni–Mo catalysts.^{17,18} Gallium-containing zeolites are known to have high catalytic activities for aromatization of light paraffins,^{19–21} NO reduction with methane,²² and aniline synthesis from phenol.²³ Because gallium oxide usually has a low surface area, Ga₂O₃ supported on γ -Al₂O₃ and γ -Ga₂O₃–Al₂O₃ solid solutions are usually preferred for catalyst use.

In the alumina–water system, four polymorphs of Al(OH)₃, gibbsite, bayerite, nordstrondite, and doyleite^{24,25}; two polymorphs of AlOOH, boehmite and diaspore, are known besides tohdite (5Al₂O₃·H₂O).²⁶ Gibbsite, bayerite, and nordstrondite can be crystallized from aqueous solutions. Although boehmite is also crystallized from aqueous media under ambient conditions, crystallization of diaspore from aqueous media usually requires high temperatures and pressures. In the gallia–water system, on the other hand, crystalline Ga(OH)₃ is not formed,^{27,28} and GaOOH having the diaspore structure is easily crystallized.^{27,29}

Synthesis of Ga–Al solid solution systems has been examined by several researchers. Hill *et al.*²⁹ reported that the boehmite solid solution extended to an approximate composition of Al_{0.7}Ga_{0.3}OOH, and Zhao *et al.*³⁰ also reported the synthesis of gallium-doped boehmite (Ga < 20%). However, synthesis of the boehmite solid solutions in the entire range from Al end to Ga end appears to be impossible because GaOOH having the boehmite structure has never been reported. On the other hand, Al_xGa_{1–x}OOH solid solutions having the diaspore structure seem to exist because both end members, AlOOH and GaOOH,

are thermodynamically stable. However, synthesis of diaspore solid solutions is extremely difficult, especially for Al-rich compositions. Actually, Hill *et al.*²⁹ reported that the samples of the gel obtained by coprecipitation from Al and Ga nitrates could not be converted to the diaspore structure when the Ga content was < 25%. Escribano *et al.*³¹ examined coprecipitation of Al and Ga nitrates with ammonia and reported that diaspore-type compounds were formed for Ga-rich compositions, whereas Al-rich precipitates were amorphous. Incorporation of Al³⁺ ions in the GaOOH structure was suggested but 12% content of Al³⁺ ions in the GaOOH (diaspore) was estimated for the precipitate obtained from 75% Ga to 25% Al composition.³¹

The γ -Ga₂O₃–Al₂O₃ solid solutions are usually prepared by impregnation of pseudoboehmite^{5,6,8} or γ -alumina^{4,32} with a solution of Ga nitrate and subsequent calcination. However, these methods do not guarantee the homogeneity of Al³⁺ and Ga³⁺ ions in Ga₂O₃–Al₂O₃ because diffusion of Ga³⁺ ions in the alumina matrix is required. As far as the authors know, the most successful synthesis of the γ -Ga₂O₃–Al₂O₃ solid solutions by the precipitation method was reported by Otero Areán *et al.*³³ who synthesized γ -Ga₂O₃–Al₂O₃ solid solutions by calcination of the amorphous gels obtained by coprecipitation from Al and Ga nitrates. They used ethanolic solutions of Al and Ga nitrates because the presence of excess water in the resulting gel leads to crystallization of GaOOH (diaspore), which is not a precursor of γ -Ga₂O₃.³⁴ However, homogeneity of Al³⁺ and Ga³⁺ ions in the precursor gel was not confirmed because of its amorphous nature.

Dawsonite is a mineralogical name for naturally occurring sodium aluminum carbonate hydroxide (NaAl(OH)₂CO₃).³⁵ Ammonium aluminum carbonate hydroxide (NH₄Al(OH)₂CO₃, AACH) is included in the group of dawsonite and is also called ammonium dawsonite. The crystal structure of AACH was determined by Iga and Kato,³⁶ who reported that it belongs to the space group of *Cmcm*. This structure is slightly different from that of dawsonite, because the space group of dawsonite (*Imma*)³⁵ cannot accommodate the ammonium ions having a *T_d* symmetry. AACH was prepared by the addition of an aluminum nitrate solution into a solution of ammonium carbonate or bicarbonate.^{37–39} This compound has been used as a suitable starting material for the synthesis of α - and γ -Al₂O₃ depending on the calcination temperature.^{39–42} As far as the authors know, only two papers have reported the formation of ammonium gallium carbonate hydroxide (AGCH).^{43,44} Sidorenko *et al.*⁴³ reported that AGCH crystallized in the *Pbcn* space group, which is different from that of AACH (*Cmcm*)³⁶.

We found that γ -Ga₂O₃–Al₂O₃ solid solutions prepared by solvothermal methods have high catalytic activities for selective catalytic reduction (SCR) of NO with methane as a reducing agent.^{7,45,46} The activity of the catalyst prepared solvothermally using various solvents depended on the crystallite size of the catalyst. The catalyst with a large crystallite size had high catalytic activity in spite of the fact that the catalyst had low surface

E. Slamovich—contributing editor

Manuscript No. 27683. Received March 19, 2010; approved June 1, 2010.

*Member, The American Ceramic Society.

[‡]Author to whom correspondence should be addressed. e-mail: inoue@scl.kyoto-u.ac.jp

area.⁴⁶ We recently found that calcination of the precursors obtained by coprecipitation of gallium and aluminum nitrates with ammonium carbonate yielded well-crystallized γ -Ga₂O₃-Al₂O₃ solid solutions, which also showed high catalytic activities for methane-SCR of NO.⁴⁷ Other precipitants resulted in the formation of catalysts with low activities. The X-ray diffraction (XRD) patterns of the precursors obtained by coprecipitation with ammonium carbonate resemble that of AACH. Therefore, solid solutions of AGCH–AACH are expected to be formed.

In the present work, therefore, we have examined optimum conditions to synthesize the Ga₂O₃-Al₂O₃ solid solutions and attention has been paid for the synthesis and structure of the AGCH–AACH solid solutions as the precursors of the oxide solid solutions.

II. Experimental Procedure

(1) Preparation of γ -Ga₂O₃-Al₂O₃ Solid Solutions

Appropriate amounts of gallium nitrate hydrate (Ga(NO₃)₃ · *n*H₂O; Mitsuwa Chemical, Osaka, Japan) and aluminum nitrate nonahydrate (Al(NO₃)₃ · 9H₂O; Nacalai Tesque, Kyoto, Japan) were dissolved in 100 mL of deionized water. This solution was added to a 200 mL solution of excess (NH₄)₂CO₃ at once at a prescribed temperature (usually 25°C) with vigorous stirring and the mixture was stirred for 1 h. The precipitate was centrifuged and washed with deionized water twice and ethanol twice followed by drying at 80°C. The precursor was calcined at 700°C for 3 h in air to yield the γ -Ga₂O₃-Al₂O₃ solid solutions.

(2) Characterization

Powder XRD patterns were obtained (Model XD-D1 Shimadzu, Kyoto, Japan) using CuK α radiation and a carbon monochromator. Crystallite size was calculated from the half-height width of the (440) diffraction peak of γ -Ga₂O₃-Al₂O₃ using the Scherrer equation. For Rietveld analysis, the XRD pattern was measured on another diffractometer (Rigaku Rint 2500, Rigaku, Tokyo, Japan) and analyzed by RIETAN-2000 program.⁴⁸ The TCH pseudovoigt profile function was used.

BET surface area was calculated using the single-point method on the basis of the nitrogen uptake measured at 77 K. The samples were pretreated in an N₂ flow at 300°C for 30 min before the measurement.

X-ray absorption fine structure (XAFS) measurements for Ga K-edge were carried out on BL14B2 beam line at SPring-8 (Harima, Japan). An Si(311) monochromator was used to monochromatize the X-ray. The absorption spectra in the Ga K-edge region were measured by the transmission mode at room temperature. The proportions of *T_d* and *O_h* gallium sites in the samples were estimated by the linear combination fitting method from their XANES data. The γ -Ga₂O₃-Al₂O₃ solid solution with the Ga/(Ga+Al) ratio of 0.1 prepared solvothermally in 2-methylaminoethanol and ZnGa₂O₄ having a normal spinel structure were used as the *T_d* and *O_h* standard samples, respectively.

III. Results and Discussion

(1) Effects of Amount of (NH₄)₂CO₃

The effects of the amount of (NH₄)₂CO₃ on the preparation of dawsonite at 25°C were reported previously.⁴⁷ The product prepared with 1.5-fold excess of (NH₄)₂CO₃ in relation to the stoichiometric amount was amorphous. However, large excess of (NH₄)₂CO₃ yielded products that exhibited the XRD patterns due to dawsonite.^{39,40,49} Note that the following stoichiometric equation was assumed for the preparation of dawsonite:

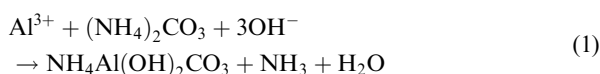


Figure 1 shows TG–DTA profiles of AGCH–AACH obtained with various amounts of (NH₄)₂CO₃ at 25°C. The

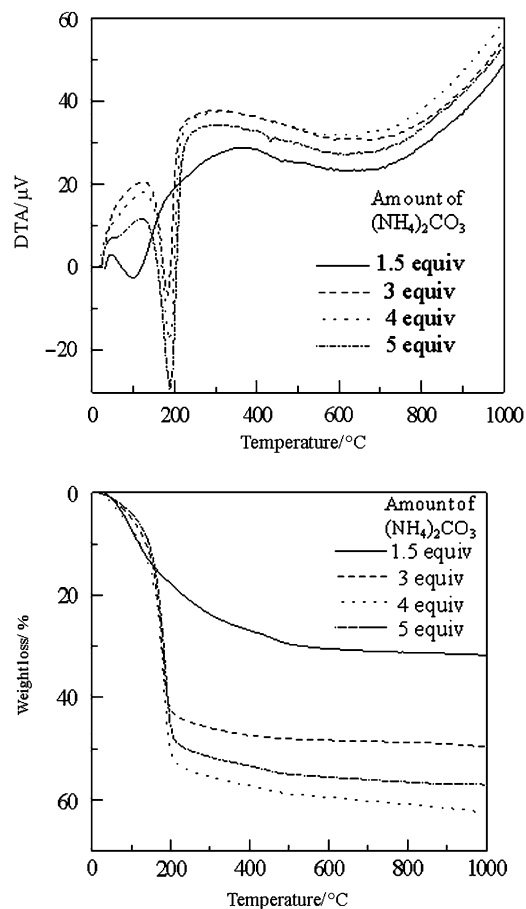


Fig. 1. TG and DTA profiles of the products obtained by coprecipitation of gallium and aluminum nitrates at 25°C with various amounts of (NH₄)₂CO₃.

TG profile of the product prepared with 1.5-fold excess of (NH₄)₂CO₃ exhibited a gradual weight decrease in a wide temperature range. This result accords with the XRD result, which showed the amorphous nature of this product. On the other hand, the TG profile of the products obtained with three to fivefold excess of (NH₄)₂CO₃ showed a sharp weight decrease at about 200°C associated with an endothermic response in DTA. Theoretical weight loss of AGCH–AACH solid solution (Ga/(Ga+Al) = 0.225) is calculated to be 59.2%. The weight losses of the products prepared with four and fivefold excess (NH₄)₂CO₃ were essentially identical with the theoretical value but weight loss of the product obtained with threefold excess (NH₄)₂CO₃ was smaller than the theoretical, indicating that this product contains a small amount of an amorphous phase.

(2) Preparation of AGCH–AACH Solid Solutions with Various Ga/Al Ratios

Figure 2 shows the XRD patterns of the products (Ga/(Ga+Al) = 0.225) obtained at various temperatures with fivefold excess of (NH₄)₂CO₃ as a precipitant. In a temperature range of 0°–80°C, the crystallinity of the dawsonite sample increased with the increase in the precipitation temperature. However, further increase in the crystallinity was not attained by prolonging the aging period from 1 to 4 h at 80°C (data not shown).

Figure 3 shows the XRD patterns of AGCH–AACH prepared at 80°C using fivefold excess of (NH₄)₂CO₃ from various charged ratios of Ga/(Ga+Al). The peak patterns of the products are almost the same as that of AACH reported in the literature.^{39,40,49} AGCH was similarly prepared from Ga(NO₃)₃ with (NH₄)₂CO₃, and its XRD pattern (Fig. 4) indicates that it has the same structure as that of AACH. With the increase in the Ga/(Ga+Al) ratio, the diffraction peaks gradually shifted

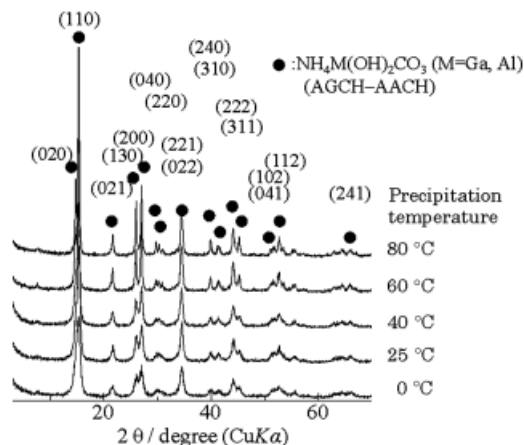


Fig. 2. X-ray diffraction patterns of the products obtained by coprecipitation of gallium and aluminum nitrates at various temperatures with fivefold excess of $(\text{NH}_4)_2\text{CO}_3$ as a precipitant.

to the lower angle side, indicating that the unit cell parameters are enlarged by incorporation of Ga^{3+} ion because the ionic size of Ga^{3+} (0.76 Å for CN 6) is larger than that of Al^{3+} (0.675 Å for CN 6). These results indicate that the AGCH–AACH solid solutions are formed in the whole range of Al–Ga composition. The XRD analyses of the dawsonites indicated that the crystallinity of the product increased with the increase in the $\text{Ga}/(\text{Ga}+\text{Al})$ ratio, just as the products obtained at 25°C.⁴⁷

Figure 4 shows the XRD patterns of AGCH–AACH prepared at 80°C using threefold excess of $(\text{NH}_4)_2\text{CO}_3$ from various charged ratios of $\text{Ga}/(\text{Ga}+\text{Al})$. The products with higher Ga contents ($\text{Ga}/(\text{Ga}+\text{Al}) \geq 0.5$) were amorphous, while dawsonite crystals were obtained for the products with lower Ga contents. Among the products obtained under this condition, AACH had the highest crystallinity. In other words, the crystallinity of dawsonite prepared at 80°C using threefold excess of $(\text{NH}_4)_2\text{CO}_3$ decreased with the increase in the $\text{Ga}/(\text{Ga}+\text{Al})$ ratio. These results indicate that the adequate amount of $(\text{NH}_4)_2\text{CO}_3$ for the preparation of highly crystallized dawsonites depends on the $\text{Ga}/(\text{Ga}+\text{Al})$ ratio and precipitation temperature.

Figure 5 shows the structures of AACH and AGCH refined using the space group of *Cmcm* and AGCH refined using the *Pbcn* space group. The crystal structures of AGCH refined using

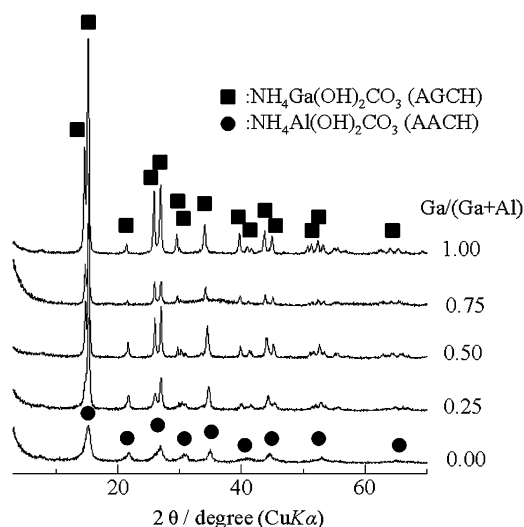


Fig. 3. X-ray diffraction patterns of AGCH–AACH samples prepared from mixtures of gallium and aluminum nitrates at 80°C with various ratios of $\text{Ga}/(\text{Ga}+\text{Al})$ by coprecipitation with fivefold excess $(\text{NH}_4)_2\text{CO}_3$.

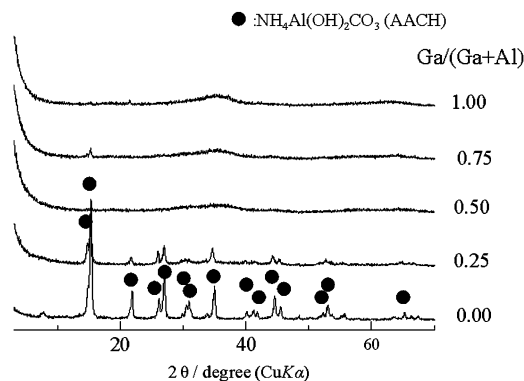


Fig. 4. X-ray diffraction patterns of AGCH–AACH samples prepared from mixtures of gallium and aluminum nitrates at 80°C with various ratios of $\text{Ga}/(\text{Ga}+\text{Al})$ by coprecipitation with threefold excess $(\text{NH}_4)_2\text{CO}_3$.

Cmcm and *Pbcn* are quite similar to each other and we could not find any reason why AGCH has a lower symmetry than AACH.

Figure 6 shows the observed, calculated, and difference profiles for the final refinement of XRD of AGCH. The empirical formula of AGCH calculated based on the *Cmcm* space group was close to the ideal one. The observed, calculated, and difference profiles for the AACH refined using *Cmcm* and AGCH using *Pbcn* are given in the supporting information (Figs. S1 and S2).

Table I shows the results of Rietveld analyses of AACH and AGCH refined with the space group of *Cmcm*. Although AGCH gave a slightly large R_{wp} , both refinements gave reasonable R_{wp} values. Table II shows the results of Rietveld analyses of AGCH–AACH with $\text{Ga}/(\text{Ga}+\text{Al}) = 0.50$ on the basis of the space group of *Cmcm*. In the 4a sites, both Al^{3+} and Ga^{3+} ions are located, indicating the formation of the AGCH–AACH solid solution.

Figure 7 shows the relationship between the starting composition for coprecipitation and unit cell parameters of the solid solution calculated by Rietveld analysis. Although the data were

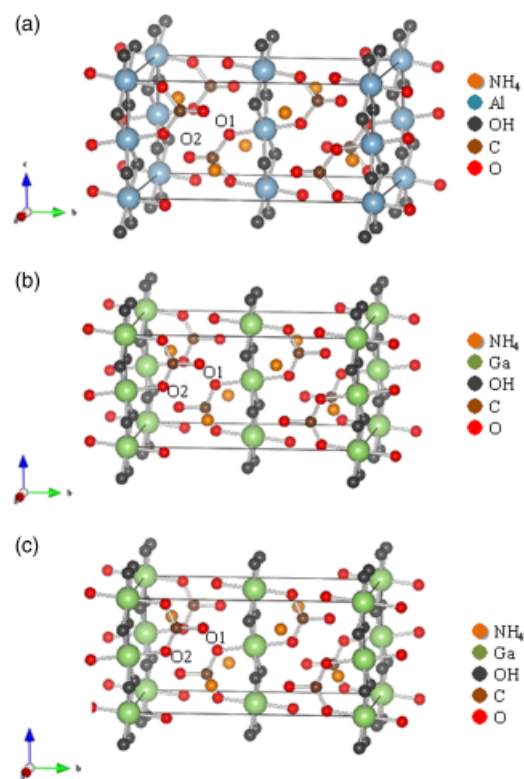


Fig. 5. Structures of (a) AACH and (b) AGCH; refined using the space group of *Cmcm* and (c) AGCH refined using *Pbcn* space group.

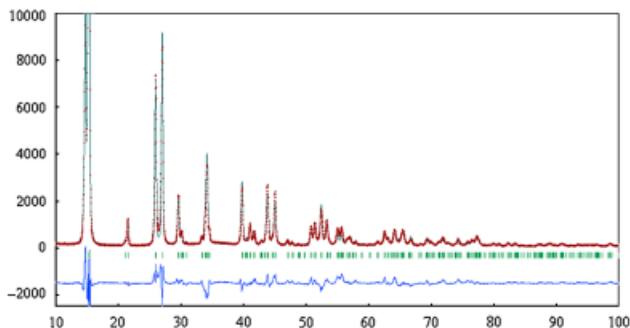


Fig. 6. Observed, calculated, and difference profiles obtained by Rietveld analysis of AGCH. The AGCH sample was prepared from a gallium nitrate solution by precipitation with fivefold excess $(\text{NH}_4)_2\text{CO}_3$ at 80°C . The profile was refined using the space group of *Cmcm*.

slightly scattered presumably because of the presence of small amounts of amorphous phase, the lattice parameters b and c were expanded, while the lattice parameter a was slightly shrunk by the incorporation of Ga^{3+} ions in the AACH structure.

Figure 8 shows IR spectra of the solid solutions with various compositions. According to the literature,^{50–53} the absorption bands of AACH ($\text{Ga}/(\text{Ga}+\text{Al}) = 0.00$) were assigned as follows: νOH , at 3423 cm^{-1} ; δOH , at 991 cm^{-1} ; νNH , at 3151 , 3007 , and 2831 cm^{-1} ; δNH , at 1839 and 1719 cm^{-1} ; $\nu\text{C-O}$ of the CO_3^{2-} groups, at 1543 , 1447 , 1380 , 759 , and 727 cm^{-1} ; and $\nu\text{Al-O}$ lattice vibration, at 1103 cm^{-1} . On the other hand, the absorption bands of AGCH ($\text{Ga}/(\text{Ga}+\text{Al}) = 1.00$) can be assigned as follows: νOH , at 3376 cm^{-1} ; δOH , at 983 cm^{-1} ; νNH , at 3155 , 3057 , and 2851 cm^{-1} ; δNH , at 1803 and 1720 cm^{-1} ; $\nu\text{C-O}$, at 1522 , 1446 , 1362 , 762 , and 709 cm^{-1} ; and $\nu\text{Ga-O}$ lattice vibration, at 1089 cm^{-1} . For the solid solutions, these bands appeared at the frequencies between those observed for AACH and AGCH and these two compounds had same numbers of absorption bands. Therefore, *Pbcn* space group having a lower symmetry can be ruled out for AGCH.

Figure 9 shows the Raman spectra of the solid solutions with various compositions. All the bands were assigned to lattice vibrations.⁵² Because the same number of Raman band was observed for AACH and AGCH, these compounds have the same symmetry and the possibility that AGCH belongs to the *Pbcn* space group can be ruled out. It is interesting to note that the band at $\sim 550\text{ cm}^{-1}$ split into two peaks when Al^{3+} and Ga^{3+} ions are present in the structure. This is the so-called “two-mode behavior”⁵⁴ and is found in the solid solution systems of metals, carbide, nitride, oxides, etc.^{55–57} The origin of the two-mode behavior is not yet fully understood, but it is known that the intensity ratio of the two peaks approximately corresponds to the composition ratio of the solid solution.^{54,55,57} Therefore, the peaks were deconvoluted and the results are given in Table III. Apparently, the intensity ratio is approximately identical with the starting composition ratio, indicating that Al^{3+} and Ga^{3+} ions are well incorporated into the structure of the solid solution at the coprecipitation stage. Although micro-segregation, which cannot be detected by XRD,^{58,59} cannot be ruled out, we believe that homogeneous solid solutions

Table II. Results for Rietveld Analysis of AGCH–AACH Obtained from $\text{Ga}/(\text{Ga}+\text{Al}) = 0.5$

Element	Site	g^\dagger	x	y	z
Ga	4a	0.394	0	0	0
Al		0.502			
C	4c	0.750	0	0.7810 (12)	0.2500
NH_4	4c	0.811	0	0.3473 (8)	0.2500
OH	8g	1.000	0.1943 (6)	0.0146 (6)	0.2500
O1	8f	0.750	0	0.8433 (4)	0.0626 (10)
O2	4c	0.750	0	0.6764 (8)	0.2500

Space group: *Cmcm* (No.63). R_{wp} : 9.98. † Site occupancy. AACH, ammonium aluminum carbonate hydroxide; AGCH, ammonium gallium carbonate hydroxide.

were formed because the two-mode behavior was not observed for other Raman bands.

Figure 10 shows the Ga K-edge XAFS spectra of the dawsonites prepared with various $\text{Ga}/(\text{Ga}+\text{Al})$ charged ratios. The peak positions for $T_d\text{-Ga}^{3+}$ and $O_h\text{-Ga}^{3+}$ (10373 and 10376 eV , respectively⁴) are shown by broken lines. As shown in Fig. 10, all the products exhibited essentially identical Ga K-edge XANES spectra, which gave a peak at the midway between the peak positions of $T_d\text{-Ga}^{3+}$ and $O_h\text{-Ga}^{3+}$. Although the metal ions in the dawsonite structure have the octahedral coordination,³⁶ dawsonite has two types of M–O bonds: two M–O–CO₂ bonds in the axial positions and four M–OH bonds in the equatorial positions. This means that the structure is tetragonally distorted, with metal ions having a D_{4h} -like environment. Note that the crystallographic symmetry of the metal sites (Wyckoff 4a sites) of the *Cmcm* space group is C_{2h} , whereas Wyckoff 4a sites of the *Pbcn* space group (Ga sites if one assumes that AGCH belongs to this space group) have C_i symmetry. In AACH, the bond length of Al–O–CO₂ calculated by Rietveld analysis is 1.88 \AA and that of Al–OH is 1.95 \AA . AGCH has a similar structure to AACH. The distorted octahedral structure of Ga^{3+} ions in AACH–AGCH would give the absorption peak at an intermediate between those of $T_d\text{-Ga}^{3+}$ and $O_h\text{-Ga}^{3+}$.

(3) Preparation and Structure of $\gamma\text{-Ga}_2\text{O}_3\text{-Al}_2\text{O}_3$ Solid Solutions with Various Ga/Al Ratios

Figure 11 shows TG–DTA profiles of the solid solutions. A sharp weight loss associated with an endothermic response in DTA was observed for all the products. This result accords with the results obtained by FT-IR, Raman spectra, and XRD patterns, which suggested that AGCH–AACH solid solutions were obtained for the entire composition from Al to Ga end members. The weight loss process is explained by the simultaneous desorption of water from hydroxide ions and of carbon dioxide from carbonate ions. Although the observed weight losses for the Ga-rich products were significantly smaller than the theoretical values, those of the Al-rich products were essentially identical with the theoretical values.

The XRD patterns of the samples obtained by calcination of the AACH–AGCH solid solutions in air at 700°C were reported previously.⁴⁷ Aluminum oxide obtained by calcination of

Table I. Results for Rietveld Analysis of Dawsonite Samples

Sample	Site occupancy							R_{wp}
	4a		4c	4c	8g	8f	4c	
	Al	Ga	C	NH_4	OH	O1	O2	
AACH	1.000	—	0.926	0.851(8)	1.000	0.926	0.926	9.38
AGCH	—	1.000	0.868	0.737(9)	1.000	0.868	0.868	16.54

Space group: *Cmcm* (No. 63). AACH, ammonium aluminum carbonate hydroxide; AGCH, ammonium gallium carbonate hydroxide.

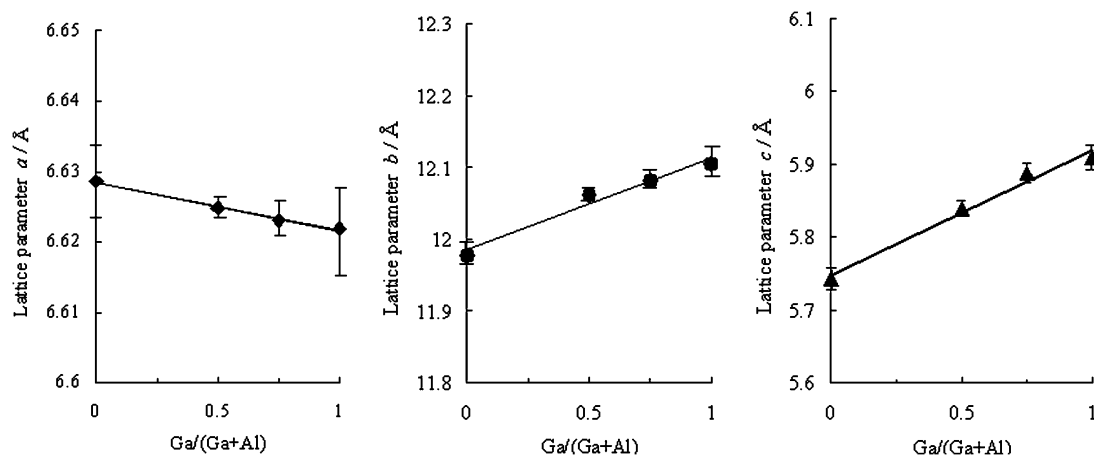


Fig. 7. Lattice parameter (a , b , and c) of the AGCH–AACH solid solutions versus Ga content in AGCH–AACH.

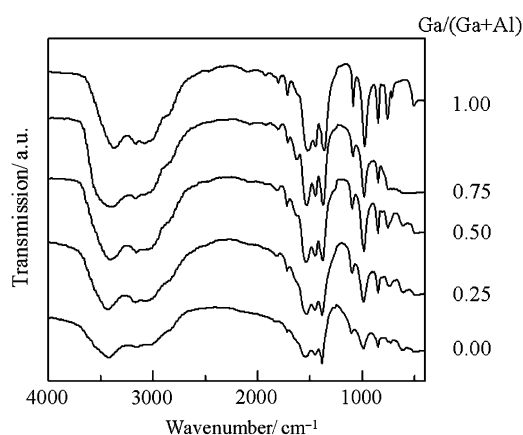


Fig. 8. IR spectra of AGCH–AACH prepared at 25°C with various ratios of Ga/(Ga+Al).

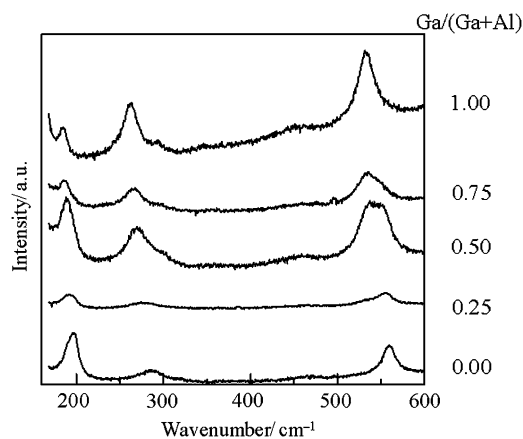


Fig. 9. Raman spectra of AGCH–AACH prepared at 25°C with various ratios of Ga/(Ga+Al).

AACH was amorphous. The samples obtained from AGCH–AACH at Ga/(Ga+Al) = 0.20–0.50 give the patterns similar to that of γ -Al₂O₃. With an increase in the Ga/(Ga+Al) ratio, the diffraction peaks gradually shifted toward the lower angle side, indicating Ga₂O₃–Al₂O₃ solid solutions were obtained.

The XRD pattern of the Ga₂O₃–Al₂O₃ mixed oxide obtained from Ga/(Ga+Al) = 0.75 indicates that partial transformation to β -Ga₂O₃-like phase occurred, and the proportion of this phase increased with the increase of the Ga/(Ga+Al) charged ratio. For the sample with Ga/(Ga+Al) = 0.75, however, the 512 peak of β -Ga₂O₃ was observed at a slightly higher angle as

Table III. Deconvolution of Raman Peaks

Ga/(Ga+Al) charged ratio	Peak position (cm ⁻¹)	Relative intensity (-)	Peak position (cm ⁻¹)	Relative intensity (-)
0	559.8	1	—	—
0.25	554.8	0.71	534.8	0.29
0.5	552.0	0.47	534.5	0.53
0.75	548.1	0.33	532.7	0.67
1	—	—	532.2	1

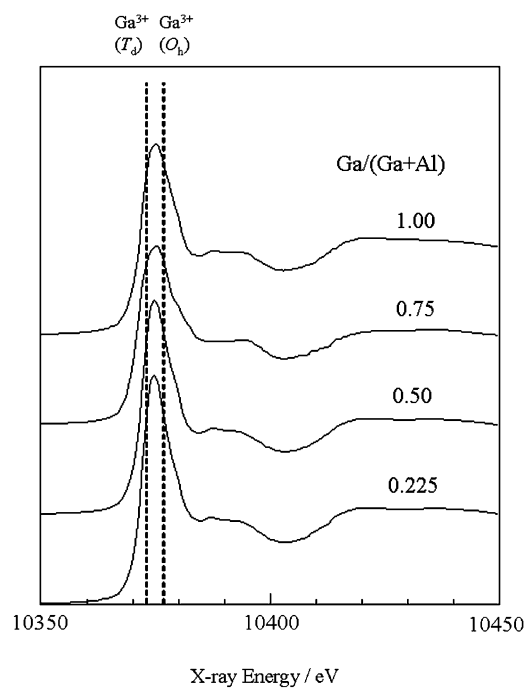


Fig. 10. Ga K-edge X-ray absorption fine structure spectra of AGCH–AACH prepared at 25°C with various ratios of Ga/(Ga+Al) by coprecipitation with (NH₄)₂CO₃.

compared with pure β -Ga₂O₃, indicating that β -Ga₂O₃- θ -Al₂O₃ solid solution was formed.

Figure 12 shows the correlation between the charged ratio of Ga and lattice parameter calculated by the XRD patterns of the Ga₂O₃–Al₂O₃ mixed oxides, which is assumed to have a cubic structure. Because the XRD pattern of the Ga₂O₃–Al₂O₃ mixed oxide obtained from Ga/(Ga+Al) = 0.75 showed β -Ga₂O₃-like

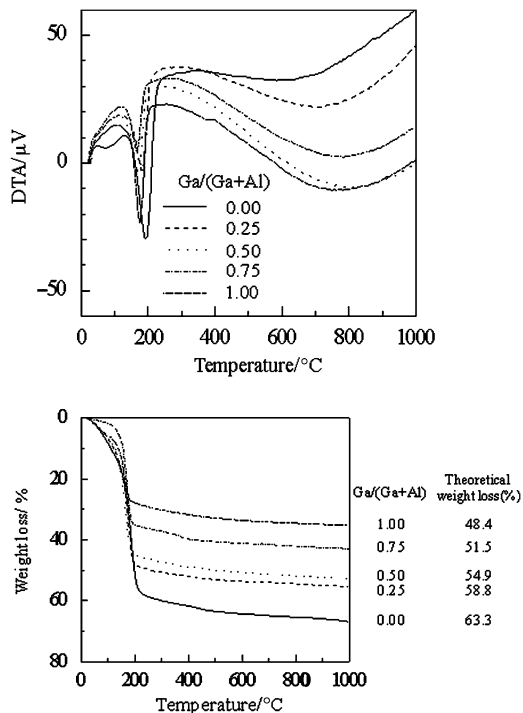


Fig. 11. TG-DTA profiles of AGCH-AACH prepared at 25°C with various ratios of Ga/(Ga+Al).

phase, its datum was not incorporated in Fig. 12. As is observed in Fig. 12, the lattice parameter increased linearly with the increase in the Ga/(Ga+Al) ratio, indicating that γ -Ga₂O₃-Al₂O₃ solid solutions were obtained by the calcination of the AGCH-AACH solid solutions. Because the precursors for the γ -Ga₂O₃-Al₂O₃ solid solutions are the AGCH-AACH solid solutions, Ga³⁺ and Al³⁺ ions must homogeneously distribute in the oxide solid solutions. In other words, homogeneous distribution of Ga³⁺ and Al³⁺ ions in AGCH-AACH was maintained in the solid solutions of γ -Ga₂O₃-Al₂O₃.

Figure 13 shows the Ga K-edge XAFS spectra of the mixed oxides prepared with various Ga/(Ga+Al) charged ratios. With the increase in the Ga/(Ga+Al) ratio, O_h-Ga³⁺ peaks clearly increased. However, Ga³⁺ ions in the solid solutions prepared with Ga/(Ga+Al) ≤ 0.50 have the T_d structure predominantly. This result suggests that Ga³⁺ ions preferentially occupy the tetrahedral sites over the octahedral sites in the defective spinel structure of the Ga₂O₃-Al₂O₃ mixed oxides.

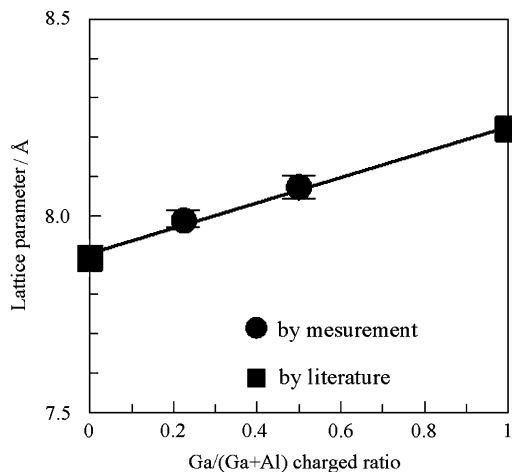


Fig. 12. Lattice parameter of the Ga₂O₃-Al₂O₃ mixed oxides versus Ga content in the Ga₂O₃-Al₂O₃ solid solutions.

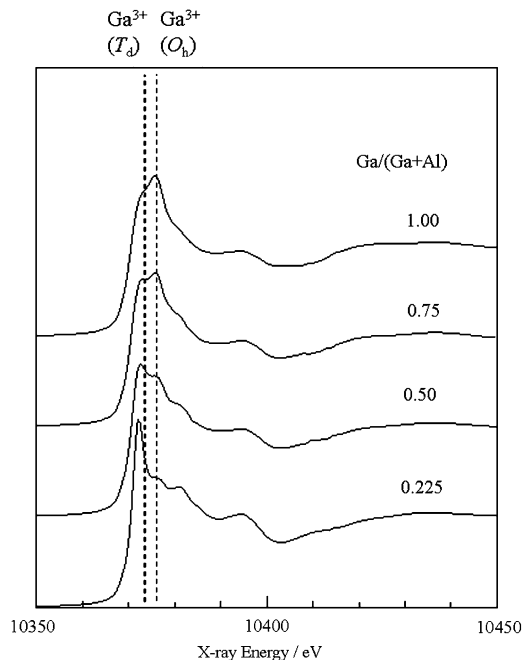


Fig. 13. Ga K-edge X-ray absorption fine structure spectra of Ga₂O₃-Al₂O₃ prepared by calcination at 700°C of AGCH-AACH solid solutions with various ratios of Ga/(Ga+Al).

Figure 14 shows the Ga K-edge XAFS spectra of AGCH-AACH prepared with Ga/(Ga+Al) = 0.50 after heating at various temperatures. Significant change of XANES spectrum was observed after calcination at 200°C. This result is consistent with TG and DTA results, which showed that AGCH-AACH was thermally decomposed at 200°C. After calcination at 200°C, both T_d and O_h structures were observed and a further increase in the calcination temperature did not alter the XANES spectra. This result indicates that the product obtained by the calcination

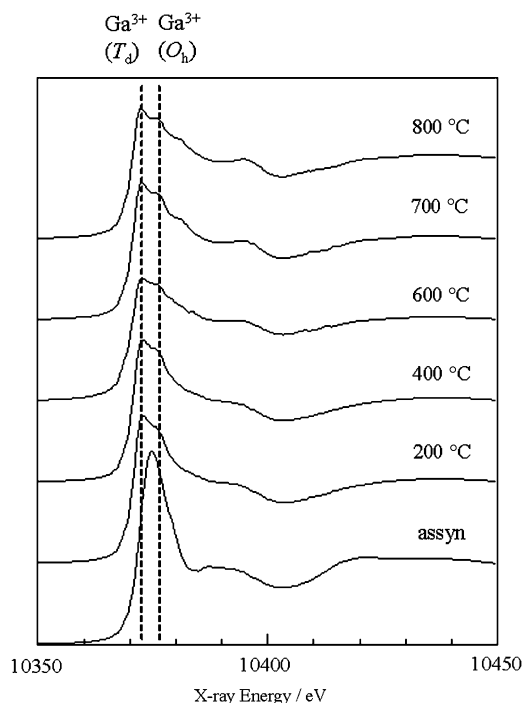


Fig. 14. Ga K-edge X-ray absorption fine structure spectra of AGCH-AACH solid solution (Ga/(Ga+Al) = 0.5) by calcination at various temperatures.

of AGCH–AACH at 200°C has a microscopic structure similar to that of the γ -Ga₂O₃–Al₂O₃ solid solution although it is X-ray amorphous.

IV. Conclusions

AGCH is isomorphous with AACH and AGCH–AACH solid solutions were prepared from aluminum and gallium nitrates with ammonium carbonate by the use of fivefold excess of ammonium carbonate. Calcination of the AACH–AGCH solid solutions prepared with $Ga/(Ga+Al) \leq 0.50$ at 700°C for 3 h gave γ -Ga₂O₃–Al₂O₃ solid solutions. Gallium ions in AGCH–AACH solid solutions were located in the distorted octahedral sites, whereas they preferentially occupied the tetrahedral sites in the defective spinel structure of the oxide solid solutions, which is the origin for high catalytic activities of the solid solutions for methane-SCR of NO. Calcination of AGCH–AACH at 200°C gave a structure similar to that of γ -Ga₂O₃–Al₂O₃, although the calcined product was X-ray amorphous.

Acknowledgments

The XAFS experiments were performed at BL14B2 in SPring-8 with the approval of the Japan Synchrotron Radiation Research Institute (JASRI) (Proposal No. 2007B1937).

Supporting Information

Additional Supporting Information may be found in the online version of this article:

Fig. S1. Observed, calculated, and difference profiles obtained by Rietveld analysis of AACH. The AACH sample was prepared from a solution of aluminum nitrate by precipitation with 5-fold excess (NH₄)₂CO₃ at 80°C. The profile was refined using the space group of *Cmcm*.

Fig. S2. Observed, calculated, and difference profiles obtained by Rietveld analysis of AGCH. The AGCH sample was prepared from a solution of gallium nitrate by precipitation with 5-fold excess (NH₄)₂CO₃ at 80°C. The profile was refined using the space group of *Pbcn*.

Please note: Wiley-Blackwell are not responsible for the content or functionality of any supporting materials supplied by the authors. Any queries (other than missing material) should be directed to the corresponding author for the article.

References

- ¹K. Nakagawa, C. Kajita, K. Okumura, N. Ikenaga, M. Nishitani-Gamo, T. Ando, T. Kobayashi, and T. Suzuki, "Role of Carbon Dioxide in the Dehydrogenation of Ethane over Gallium-Loaded Catalysts," *J. Catal.*, **203**, 87–93 (2001).
- ²B. Zheng, W. Hua, Y. Yue, and Z. Gao, "Dehydrogenation of Propane to Propene over Different Polymorphs of Gallium Oxide," *J. Catal.*, **232**, 143–51 (2005).
- ³J. A. Moreno and G. Poncelet, "Isomerization of *n*-Butane over Sulfated Al- and Ga-Promoted Zirconium Oxide Catalysts. Influence of Promoter and Preparation Method," *J. Catal.*, **203**, 453–65 (2001).
- ⁴K. Shimizu, M. Takamatsu, K. Nishi, H. Yoshida, A. Satsuma, T. Tanaka, S. Yoshida, and T. Hattori, "Alumina-Supported Gallium Oxide Catalysts for NO Selective Reduction: Influence of the Local Structure of Surface Gallium Oxide Species on the Catalytic Activity," *J. Phys. Chem. B*, **103** [9] 1542–9 (1999).
- ⁵M. Haneda, Y. Kintaichi, T. Mizushima, N. Kakuta, and H. Hamada, "Structure of Ga₂O₃–Al₂O₃ Prepared by Sol-Gel Method and Its Catalytic Performance for NO Reduction by Propene in the Presence of Oxygen," *Appl. Catal. B: Environ.*, **31**, 81–92 (2001).
- ⁶T. Horiuchi, L. Chen, T. Osaki, and T. Mori, "Thermally Stable Alumina–Gallia Aerogel as a Catalyst for NO Reduction with C₃H₆ in the Presence of Oxygen," *Catal. Lett.*, **72** [1–2] 77–81 (2001).
- ⁷M. Takahashi, N. Inoue, T. Nakamura, T. Takeguchi, S. Iwamoto, T. Watanabe, and M. Inoue, "Selective Catalytic Reduction of NO with Methane on γ -Ga₂O₃–Al₂O₃ Solid Solutions Prepared by the Solvothermal Method," *Appl. Catal. B: Environ.*, **65**, 142–9 (2006).
- ⁸Z. M. El-Bahy, R. Ohnishi, and M. Ichikawa, "Hydrolytic Decomposition of CF₄ Over Alumina-Based Binary Metal Oxide Catalysts: High Catalytic Activity of Gallia–Alumina Catalyst," *Catal. Today*, **90**, 283–90 (2004).

- ⁹P. P. Pescarmona, K. P. F. Janssen, and P. A. Jacobs, "Novel Transition-Metal-Free Heterogeneous Epoxidation Catalysts Discovered by Means of High-Throughput Experimentation," *Chem. Eur. J.*, **13**, 6562–72 (2007).
- ¹⁰K. Ikarashi, J. Sato, H. Kobayashi, H. Saito, N. Nishiyama, and Y. Inoue, "Photocatalysis for Water Decomposition by RuO₂-Dispersed ZnGa₂O₄ with d¹⁰ Configuration," *J. Phys. Chem. B*, **106** [35] 9048–53 (2002).
- ¹¹Y. Hou, L. Wu, X. Wang, Z. Ding, Z. Li, and X. Fu, "Photocatalytic Performance of α -, β -, and γ -Ga₂O₃ for the Destruction of Volatile Aromatic Pollutants in Air," *J. Catal.*, **250**, 12–8 (2007).
- ¹²F. Domínguez, J. Sánchez, G. Artega, and E. Choren, "Gallia as Support of Pt in Benzene Hydrogenation Reaction," *J. Mol. Catal. A: Chem.*, **228**, 319–24 (2005).
- ¹³S. E. Collins, M. A. Baltanás, and A. L. Bonivardi, "An Infrared Study of the Intermediates of Methanol Synthesis from Carbon Dioxide over Pd/ β -Ga₂O₃," *J. Catal.*, **226**, 410–21 (2004).
- ¹⁴N. Iwasa, T. Mayanagi, W. Nomura, M. Arai, and N. Takezawa, "Effect of Zn Addition to Supported Pd Catalysts in the Steam Reforming of Methanol," *Appl. Catal. A: General*, **248**, 153–60 (2003).
- ¹⁵N. Iwasa, T. Mayanagi, N. Ogawa, K. Sakata, and N. Takezawa, "New Catalytic Functions of Pd–Zn, Pd–Ga, Pd–In, Pt–Zn, Pt–Ga and Pt–In Alloys in the Conversions of Methanol," *Catal. Lett.*, **54**, 119–23 (1998).
- ¹⁶T. Fujitani, M. Saito, Y. Kanai, T. Watanabe, J. Nakamura, and T. Uchijima, "Development of an Active Ga₂O₃ Supported Palladium Catalysts for the Synthesis of Methanol from Carbon Dioxide and Hydrogen," *Appl. Catal. A: General*, **125**, L199–202 (1995).
- ¹⁷T. Olorunyolemi and R. Kydd, "Gallium–Aluminum Mixed Oxides as Supports for Ni–Mo Catalysts: Characterization and Reactivity for Cumene Cracking and Thiophene HDS Reactions," *J. Catal.*, **158**, 583–6 (1996).
- ¹⁸T. Olorunyolemi and R. A. Kydd, "Laser Raman Spectroscopy of MoO₃ and Ni–MoO₃ Supported on Gallia and Gallium–Aluminum Mixed Oxides," *Catal. Lett.*, **65**, 185–92 (2000).
- ¹⁹G. D. Meitzner, E. Iglesia, J. E. Baumgartner, and E. S. Huang, "The Chemical State of Gallium in Working Alkane Dehydrocyclodimerization Catalysts. *In Situ* Gallium K-Edge X-Ray Absorption Spectroscopy," *J. Catal.*, **140**, 209–25 (1993).
- ²⁰R. Carli, R. L. van Mao, C. Bianchi, and V. Ragaini, "Hydrogen Sorption Sites in the Gallium Containing Hybrid Catalysts Used for the Aromatization of Light Alkanes," *Catal. Lett.*, **21**, 265–74 (1993).
- ²¹R. L. van Mao, J. Yao, L. A. Dufresne, and R. Carli, "Hybrid Catalysts Containing Zeolite ZSM-5 and Supported Gallium Oxide in the Aromatization of *n*-Butane," *Catal. Today*, **31**, 247–55 (1996).
- ²²Y. Li and J. N. Armor, "Selective Catalytic Reduction of NO with methane on Gallium Catalysts," *J. Catal.*, **145**, 1–9 (1994).
- ²³N. Katada, S. Kuroda, and M. Niwa, "High Catalytic Activity for Synthesis of Aniline from Phenol and Ammonia Found on Gallium-Containing MFI," *Appl. Catal. A: General*, **180**, L1–3 (1999).
- ²⁴G. R. Clark, K. A. Rodgers, and G. S. Henderson, "The Crystal Chemistry of Doyleite, Al(OH)₃," *Z. Kristallogr.*, **213** [2] 96–100 (1998).
- ²⁵H. Liu, J. Hu, J. Xu, Z. Liu, J. Shu, H. K. Mao, and J. Chen, "Phase Transition and Compression Behavior of Gibbsite under High-Pressure," *Phys. Chem. Minerals*, **31**, 240–6 (2004).
- ²⁶K. Wefers, "Nomenclature, Preparation, and Properties of Aluminum Oxides, Oxide Hydroxides, and Trioxides"; pp. 13–22 in *Alumina Chemicals: Science and Technology Handbook*, Edited by L. D. Hart. The American Ceramic Society, Westerville, OH, 1990.
- ²⁷R. Roy, V. G. Hill, and E. F. Osborn, "Polymorphism Ga₂O₃ and the System Ga₂O₃–H₂O," *J. Am. Chem. Soc.*, **74** [2] 719–22 (1952).
- ²⁸S. M. Bradley, R. A. Kydd, and R. Yamdagni, "Detection of a New Polymeric Species Formed through the Hydrolysis of Gallium(III) Salt Solution," *J. Chem. Soc., Dalton Trans.*, 413–7 (1990).
- ²⁹V. G. Hill, R. Roy, and E. F. Osborn, "The System Alumina–Gallia–Water," *J. Am. Ceram. Soc.*, **35** [6] 135–42 (1952).
- ³⁰Y. Zhao, R. L. Frost, and W. N. Martens, "Gallium-Doped Boehmite Nanotubes and Nanoribbons. A TEM, EDX, XRD, BET, and TG Study," *J. Phys. Chem. C*, **111** [14] 5313–24 (2007).
- ³¹V. S. Escrivano, J. M. G. Amores, E. F. López, M. Panizza, C. Resini, and G. Busca, "Solid State Characterization of Coprecipitated Alumina–Gallia Mixed Oxide Powders," *J. Mater. Sci.*, **40**, 2013–21 (2005).
- ³²Yu. N. Pushkar, A. Sintsy, O. O. Parenago, A. N. Kharlanov, and E. V. Lunina, "Structure and Lewis Acid Properties of Gallia–Alumina Catalysts," *Appl. Surf. Sci.*, **167**, 69–78 (2000).
- ³³C. Otero Areán, M. Rodríguez Delgado, V. Montouillout, and D. Massiot, "Synthesis and Characterization of Spinel-Type Gallia–Alumina Solid Solutions," *Z. Anorg. Allg. Chem.*, **631**, 2121–6 (2005).
- ³⁴C. Otero Areán, A. López Bellan, M. P. Mentrui, M. Rodríguez Delgado, and G. T. Palomino, "Preparation and Characterization of Mesoporous γ -Ga₂O₃," *Micropor. Mesopor. Mater.*, **40**, 35–42 (2000).
- ³⁵A. F. Frueh Jr. and J. P. Golightly, "The Crystal Structure of Dawsonite NaAl(CO₃)(OH)₂," *Canad. Mineralog.*, **9**, 51–6 (1967).
- ³⁶T. Iga and S. Kato, "Crystal Structure of NH₄-Dawsonite," *J. Ceram. Soc. Jpn.*, **86** [11] 509–13 (1978).
- ³⁷S. Kato, T. Iga, S. Hatano, and Y. Isawa, "Synthesis of NH₄Al(OH)HCO₃," *J. Ceram. Soc. Jpn.*, **84** [5] 215–20 (1976).
- ³⁸C. C. Ma, X.-X. Zhou, X. Xu, and T. Zhu, "Synthesis and Thermal Decomposition of Aluminum Carbonate Hydroxide (AACH)," *Mater. Chem. Phys.*, **72**, 374–9 (2001).
- ³⁹Z. Li, X. Feng, and H. Yao, "Ultrafine Alumina Powders Derived from Ammonium Aluminum Carbonate Hydroxide," *J. Mater. Sci.*, **39**, 2267–9 (2004).

- ⁴⁰K. Morinaga, T. Torikai, K. Nakagawa, and S. Fujino, "Fabrication of Fine α -Alumina Powders by Thermal Decomposition of Ammonium Aluminum Carbonate Hydroxide (AACH)," *Acta Mater.*, **48**, 4735–41 (2000).
- ⁴¹T. Iga and Y. Murase, "Preparation of Acicular Particles of α -Alumina," *J. Mater. Sci.*, **10** [7] 1579–81 (1995).
- ⁴²M. Giannos, M. Hoang, and T. W. Turney, "Thermally Stable Aluminas for High Temperature Applications," *Chem. Lett.*, **27**, 793–4 (1998).
- ⁴³T. D. Sidorenko, S. N. Grishaeva, and Y. G. Dorokhov, "Physicochemical Study of Ammonium Carbonatogallate," *Russ. J. Inorg. Chem.*, **24**, 661–2 (1979).
- ⁴⁴Z. Luo, M. Lu, J. Bao, W. Liu, and C. Gao, "Co-precipitation Synthesis of Gadolinium Gallium Garnet Powders Using Ammonium Hydrogen Carbonate as the Precipitant," *Mater. Lett.*, **59**, 1188–91 (2005).
- ⁴⁵M. Takahashi, N. Inoue, T. Takeguchi, S. Iwamoto, M. Inoue, and T. Watanabe, "Synthesis of γ -Ga₂O₃-Al₂O₃ by the Glycothermal Method," *J. Am. Ceram. Soc.*, **89**, 2158–66 (2006).
- ⁴⁶M. Takahashi, T. Nakatani, S. Iwamoto, T. Watanabe, and M. Inoue, "Effect of Modification by Alkali on the γ -Ga₂O₃-Al₂O₃ Mixed Oxides Prepared by the Solvothermal Method," *J. Phys.: Condens. Matter.*, **18**, 5745–57 (2006).
- ⁴⁷T. Masuda, T. Watanabe, Y. Miyahara, H. Kanai, and M. Inoue, "Synthesis of Ga₂O₃-Al₂O₃ Catalysts by a Coprecipitation Method for CH₄-SCR of NO," *Top. Catal.*, **52**, 699–706 (2009).
- ⁴⁸F. Izumi and T. Ikeda, "Rietveld-Analysis Program RIETAN-98 and Its Applications to Zeolites," *Mater. Sci. Forum*, **321–3**, 198–203 (2000).
- ⁴⁹X. Sun, J. Li, F. Zhang, X. Qin, Z. Xiu, H. Ru, and J. You, "Synthesis of Nanocrystalline α -Al₂O₃ Powders from Nanometric Ammonium Aluminum Carbonate Hydroxide," *J. Am. Ceram. Soc.*, **86** [8] 1321–25 (2003).
- ⁵⁰C. J. Serna, J. V. García-Ramos, and M. J. Peña, "Vibration Study of Dawsonite Type Compounds MAl(OH)₂CO₃ (M = Na, K, NH₄)," *Spectrochim. Acta*, **41A** [5] 697–702 (1985).
- ⁵¹A. A. Ali, M. A. Hasan, and M. I. Zaki, "Dawsonite-Type Precursors for Catalytic Al, Cr, and Fe Oxides: Synthesis and Characterization," *Chem. Mater.*, **17** [26] 6797–804 (2005).
- ⁵²G. Stoica and J. Pérez-Ramírez, "Reforming Dawsonite by Memory Effect of AACH-Derived Aluminas," *Chem. Mater.*, **19** [19] 4783–90 (2007).
- ⁵³R. L. Frost and J. M. Bouzaid, "Raman Spectroscopy of Dawsonite NaAl(CO₃)(OH)₂," *J. Raman Spect.*, **38**, 873–9 (2007).
- ⁵⁴I. F. Chang and S. S. Mitra, "Long Wavelength Optical Phonons in Mixed Crystals," *Adv. Phys.*, **20**, 359–404 (1971).
- ⁵⁵I. F. Chang and S. S. Mitra, "Application of a Modified Random-Element-Isodisplacement Model to Long-Wavelength Optic Phonons of Mixed Crystals," *Phys. Rev.*, **172** [3] 924–33 (1968).
- ⁵⁶F. Bechstedt and H. Grille, "Lattice Dynamics of Ternary Alloys," *Phys. Status Solid B: Basic Res.*, **216**, 761–8 (1999).
- ⁵⁷T.-T. Kang, A. Hashimoto, and A. Yamamoto, "Raman Scattering of Indium-Rich Al_xIn_{1-x}N: Unexpected Two-Mode Behavior of A₁(LO)," *Phys. Rev. B*, **79**, 033301, 4pp (2009).
- ⁵⁸P. Parisiades, D. Lampakis, D. Palles, E. Liarokapis, and J. Karpinski, "The Relation of the Broad Band with the E_{2g} Phonon and Superconductivity in the Mg(B_{1-x}C_x)₂ Compound," *J. Magn. Magn. Mater.*, **310**, e110–2 (2007).
- ⁵⁹P. Parisiades, D. Lampakis, D. Palles, E. Liarokapis, N. D. Zhigadlo, S. Katrych, and J. Karpinski, "Two-Mode Behavior for the E_{2g} Broad Band in Mg(B_{1-x}C_x)₂," *Physica C*, **468**, 1064–9 (2008). □